Journal of Agricultural Engineering

https://www.agroengineering.org/

A low-cost AI-based sensing approach to quantify ammonia volatilization as a driver of indirect greenhouse gas emissions

Ünal Kızıl,[1] Cafer Türkmen,[2] Yakup Çıkılı,[2] Sait Can Yücebaş,[3] Ali Sümer[2]

[1]Department of Agricultural Structures and Irrigation, Faculty of Agriculture;
[2]Department of Soil Science and Plant Nutrititon Faculty of Agriculture;
[3]Department of Computer Engineering, Faculty of Engineering, Çanakkale Onsekiz Mart University, Çanakkale, Turkey

Corresponding author: Ünal Kızıl, Department of Agricultural Structures and Irrigation, Faculty of Agriculture, Çanakkale Onsekiz Mart University, Çanakkale, Turkey. E-mail: unal@comu.edu.tr

Please cite this article as doi: 10.4081/jae.2026.2097

Submitted: 12 January 2026
Accepted: 5 june 2026

A low-cost AI-based sensing approach to quantify ammonia volatilization as a driver of indirect greenhouse gas emissions

Ünal Kızıl,[1] Cafer Türkmen,[2] Yakup Çıkılı,[2] Sait Can Yücebaş,[3] Ali Sümer[2]

[1]Department of Agricultural Structures and Irrigation, Faculty of Agriculture;
[2]Department of Soil Science and Plant Nutrititon Faculty of Agriculture;
[3]Department of Computer Engineering, Faculty of Engineering, Çanakkale Onsekiz Mart University, Çanakkale, Turkey

Corresponding author: Ünal Kızıl, Department of Agricultural Structures and Irrigation, Faculty of Agriculture, Çanakkale Onsekiz Mart University, Çanakkale, Turkey. E-mail: unal@comu.edu.tr

Contributions: Ünal Kızıl, Cafer Türkmen, conceptualization. **Ünal Kızıl, Sait Can Yücebaş,** experiment software. **Cafer Türkmen, Yakup Çıkılı, Ali Sümer**, laboratory analysis. **Sait Can Yücebaş**, data analysis. **Ünal Kızıl**, writing – original drafting. **Cafer Türkmen**, project administration, funding acquisition. All authors read and approved the final version of the manuscript and agreed to be accountable for all aspects of the work.

Conflict of interest: the authors declare that there are no known competitive economic interests or personal relationships that affect the work reported in this article.

Availability of data and materials: all data generated or analyzed during this study are included in this published article.

Acknowledgements: this study was supported by The Scientific and Technological Research Council of Turkey (TÜBİTAK) with Project no: 124E374.

Abstract

This study presents the development of a low-cost, portable, and AI-enhanced electronic nose (e-nose) system for quantifying ammonia (NH_3) volatilization from fertilized agricultural soils, with a specific emphasis on its implications for indirect greenhouse gas concentrations. Although NH_3 is not a greenhouse gas itself, its volatilization contributes significantly to indirect nitrous oxide (N_2O) emissions, one of the most potent GHGs regulated under IPCC guidelines. The proposed system integrates a MICS-6814 metal oxide sensor, ESP32 microcontroller, cloud-based data transfer, and machine learning algorithms to provide real-time monitoring and predictive analysis of NH_3 losses. Time-series sensor data were normalized, converted into area-under-the-curve (AUC) metrics, and modeled using eight machine learning algorithms. After preprocessing and hyperparameter tuning, Gradient Boosting achieved the highest performance (R^2 = 0.84; MAE=0.86). Laboratory evaluations demonstrated strong correlations between AUC values and NH_3-N measurements obtained through classical boric acid trapping, validating the system's accuracy. The findings confirm that rapid detection of NH_3 volatilization can support digital nitrogen management strategies, reduce fertilizer-derived nitrogen losses, and ultimately help mitigate indirect N_2O emissions by minimizing surplus reactive nitrogen in agricultural fields. By enabling real-time emission monitoring through a low-cost digital platform, this research contributes to emerging precision agriculture solutions aimed at reducing the environmental footprint of nitrogen fertilization.

Keywords: electronic nose; ammonia concentration; machine learning; cloud database; gas sensors.

Introduction

Fertilizers applied to maintain productivity in agricultural production are the most important inputs that supplement the soil's nutrient reserves. Nitrogen (N), one of the macronutrients, is vital for plants because it is a component of amino acids, proteins, nucleic acids, chlorophyll, and various coenzymes (Okur, 2021). It is also one of the most fundamental elements that determine vegetative growth by directly affecting plants' photosynthetic ability. If nutrients lost from the soil because of crop production are not replenished, the soil's mineral and organic matter content decreases, leading to yield reductions (Polat, 2018). Therefore, sustainable crop production is possible by applying the depleted plant nutrients to the soil at the appropriate time and in the right amounts.

While organic matter is the main source of nitrogen in soils, a significant portion of Turkey's soils are deficient in organic matter (Polat *et al*., 2013). Therefore, N is an element that must be replenished annually. Synthetic nitrogen fertilizers are used to meet this need. In 2024, the global urea market was valued at $ 52.7 billion, with projections to reach $ 60.2 billion by 2033 (IMARC, 2024). In Turkey, the total consumption of chemical fertilizers reached 7.03 million tons in 2023, and nitrogen (N) fertilizers accounted for approximately 68.9% of total plant nutrient use (TAGEM, 2024).

While the widespread use of nitrogenous fertilizers contributes to increased yields, it also creates significant environmental problems. Only approximately 50% of the nitrogen applied to the soil can be taken up by plants, while the remainder is lost through leaching or gasification, and these losses correspond to an economic loss of approximately $ 17.7 billion per year (Brentrup and Palliere, 2011). A large portion of these losses is released into the atmosphere through ammonia (NH_3) volatilization that occurs after fertilization. Terman (1980) reported that nitrogen losses in the form of NH_3 from ammonium fertilizers can reach 30-70% of the applied fertilizer, while Torello *et al*. (1983) reported that these losses were between 5-10% under field conditions. Similarly, Rochette *et al*. (2009) stated that 10-45% of total nitrogen was lost as gas within 10 days from surface-applied urea fertilizer. Wang *et al*. (2021) also determined that cumulative NH_3-N loss in rice fields accounts for 9-60% of total nitrogen. These findings demonstrate that ammonia volatilization is a significant loss from both economic and environmental perspectives.

Ammonia volatilization from fertilized and manure-amended soils is a major way of reactive nitrogen loss and an indirect source of nitrous oxide (N_2O). The 2006 IPCC Guidelines treat NH_3 and NO_x volatilized from managed soils as precursors of indirect N_2O via atmospheric deposition and subsequent nitrification–denitrification (IPCC, 2006). Experimental studies show that redeposited NH_3-derived nitrogen can generate indirect N_2O fluxes (Redding *et al*., 2016; Alfaro *et al*., 2018).

Reliable quantification of ammonia (NH_3) losses from soils requires distinguishing between concentration monitoring and emission measurement. While concentration measurements describe NH_3 levels in air or chamber headspace, emission measurements quantify the flux of NH_3 from soil to the atmosphere. This distinction is critical, as the choice of instrumentation and methodology depends on it (Insausti *et al*., 2020; Li *et al*. 2023).

For NH_3 emission measurement several methods are available. Micrometeorological techniques are considered the most reliable at field scale, as they operate under natural conditions and measure emissions over large areas (Denmead, 2008). However, these methods require

advanced instruments and complex experimental setups. For smaller scale applications and comparative studies, static or dynamic chambers and wind tunnels are generally preferred (Sintermann *et al*., 2012; Götze *et al*., 2025). .

Ammonia concentration monitoring relies on different technologies, including electrochemical sensors, metal oxide semiconductor (MOS) sensors, photoacoustic analyzers, laser-based systems, and passive samplers (Insausti *et al*., 2020; Wang *et al*., 2024). High-end spectroscopic methods offer superior sensitivity and selectivity, whereas low-cost sensors enable portable and real-time applications but are more sensitive to environmental conditions such as humidity and temperature. Therefore, proper calibration and validation are essential, particularly in agricultural environments (Li *et al*., 2023).

This study lies at the intersection of these approaches. Rather than replacing reference micrometeorological methods, it proposes a low-cost, chamber-based sensing system to estimate NH_3 volatilization under controlled conditions. By combining sensor measurements with a conventional trapping method and machine learning, the study aims to translate NH_3 concentration signals into a practical indicator of ammonia volatilization, supporting scalable nitrogen management applications.

In this context, this study aims to develop and evaluate a low-cost, AI-assisted electronic nose system for monitoring ammonia dynamics from fertilized soils under controlled conditions. Unlike conventional flux-based approaches, the proposed system focuses on headspace NH_3 concentration measurements within a closed chamber, where concentration dynamics are interpreted as a proxy for ammonia volatilization intensity. Accordingly, the study addresses the following research questions: i) whether time-series responses from MOS-based sensors can be transformed into a reliable proxy indicator of ammonia volatilization; ii) to what extent machine learning models can establish robust relationships between sensor-derived features (e.g., AUC) and cumulative NH_3–N measurements obtained by reference methods;, and iii) whether such a system can provide a rapid, repeatable, and cost-effective tool for comparative analysis. The system is primarily intended for laboratory and controlled-environment applications, rather than direct field-scale flux quantification; however, its IoT-based architecture provides a scalable foundation for future adaptation to precision agriculture and distributed sensing systems.

Material and Methods

Electronic nose design

The sensors used consist of one MICS-6814 metal oxide gas sensor (MOS) (SGX Sensortech, Corcelles-Cormondrèche, Switzerland) with low electrical conductivity in clean air and one SHT11 temperature/humidity sensor (Sensirion AG, Eggbühlstr., Zürich, Switzerland). Technical specifications of the sensors are provided in Table 1.

In this study, a conventional calibration procedure (i.e., conversion of sensor signal to absolute NH_3 concentration using predefined calibration gases or standards) was not applied. Instead, the raw sensor response was used directly. The rationale for this approach is that the objective of the study was not to obtain absolute NH_3 concentration values from the sensor, but to establish a relationship between the sensor response pattern and cumulative NH_3 measurements obtained using the boric acid trapping method.

The time-series sensor data were transformed into a single quantitative descriptor using the area under the curve (AUC). Since both calibrated and non-calibrated sensor responses preserve the same relative signal dynamics, applying a calibration step prior to AUC computation would not alter the overall relationship between AUC values and ammonia measurements.

Therefore, the calibration step was replaced by a data-driven modeling approach, in which machine learning algorithms were used to map sensor-derived AUC values directly to laboratory-measured NH_3 quantities. In this sense, the machine learning model functions as an implicit calibration framework.

The temperature/humidity sensor was used to monitor temperature and relative humidity variations within the sensor chamber, enabling instantaneous detection of system malfunctions. Temperature and relative humidity are known to significantly affect MOS sensor responses. In this study, these environmental parameters were continuously monitored using the SHT11 sensor during all measurements. Experiments were conducted under controlled laboratory conditions to minimize variability in temperature and humidity. Instead of applying an explicit compensation model, the influence of these environmental factors was addressed through a combination of controlled experimental conditions, signal preprocessing (baseline correction and normalization), and data-driven modeling. Since the machine learning algorithms were trained on sensor data collected under these conditions, the resulting models implicitly account for the combined effects of ammonia concentration, temperature, and humidity on the sensor response.

The MOS gas sensors are the most used sensors in e-nose designs. In these types of gas sensors, as the detectable gas concentration increases, the conductivity of the active element increases

accordingly. To this end, pre-packaged modules purchased with the sensors are used to convert the gas response generated by the sensors into an output signal and to determine the resulting sensor responses.

The developed e-nose system converts sensor resistance changes into analog voltage signals using internal control circuits. Designed for independent operation without a computer, it utilizes Android-based smartphones for data transmission, storage, and processing through an integrated microprocessor board. Although the initial design considered an Arduino Nano, the ESP32 board was selected for its advanced performance and internet connectivity. Standard socket connections were implemented to ensure reliable assembly and easy part replacement, minimizing model errors and improving accuracy. Production and assembly standards were refined through iterative testing to optimize performance. Additionally, a Bluetooth module enables seamless communication between the prototype and smartphones for control and real-time data transfer. The microprocessor unit and the communication mechanism of the connected devices in the electronic nose prototype are schematized in Figure 1a. The operating device is also shown in Figure 1b.

Development of the data collection application

The developed e-nose system required software in three main areas. The first was embedded software on the Arduino microcontroller, responsible for converting sensor outputs into millivolt values. This software was written in C/C++ using the Arduino Integrated Development Environment (IDE), which compiles executable code into a hexadecimal text file and uploads it to the microcontroller's firmware. The processed data is then transferred to the ESP32 board for further handling and communication with a mobile application.

To collect and manage sensor data, a dedicated Android-based data collection application was developed. This app enables the transfer of collected data in CSV format to a computer for machine learning analysis. Built around the ESP32's capabilities, the system integrates wireless network configuration and real-time monitoring of environmental sensor data without requiring a fixed connection or computer interface. Users can connect directly to the system through a built-in access point and configure network settings easily, enhancing portability, usability, and flexibility in field operations.

The software leverages the ESP32's built-in Wi-Fi and web server functions using the WiFi.h, WebServer.h, DNSServer.h, and ESPmDNS.h libraries to manage network connections, DNS routing, and local domain access. If no Wi-Fi connection is detected on startup, the device activates a Captive Portal named "E-Burun_Config," allowing users to enter their desired

network credentials via a smartphone or computer. Once connected, the ESP32 launches a local web server accessible via the device's IP address or http://e-burun.local, where users can view real-time temperature, humidity, and ammonia sensor data.

The system's Automatic Test mode records measurements at one-second intervals for a set duration, saving data as CSV files containing time, ammonia concentration, temperature, and humidity. Users can stop or reset tests through the web interface and download collected data for analysis. This flexible, stand-alone system ensures reliable, field-ready data acquisition for nitrogen concentration monitoring.

Development of the Android-based mobile phone application

A second mobile phone application has been developed to estimate ammonia release at the ppm level following the sniffing of soil samples using the machine learning algorithm. The platform used for application development was developed by Google and launched by the Massachusetts Institute of Technology under the name MIT App Inventor. The platform, later updated and released as MIT App Inventor 2, offers a free application development tool. Allowing users to develop applications for the Android operating system using block coding (Wikipedia, 2021), the platform utilizes the MIT App Inventor 2 web browser.

The Android operating system is based on the Linux kernel, meaning application isolation, file system, and security rules are specific to Linux (Pocatilu, 2011). Android application files are provided as packaged files with the apk extension, which contains all the resources for the application (Burnette, 2010). Android applications are written in the Java programming language but are not executed using the standard Java Virtual Machine (JVM). Instead, Google created a dedicated virtual machine called the Dalvik VM. Here, Java is solely responsible for converting and executing the bytecode (Holla and Katti, 2012).

Data collection, processing, and modeling processes are performed in three stages. In the first stage, as explained above, the development of an application compatible with Android operating systems, which controls the device, visualizes the data flow used, and shows the classification result made by artificial intelligence, was achieved (Figure 2).

In the user interface, a Bluetooth connection is first established between the e-nose and the mobile application. The user then enters the sample name and sniffing duration before clicking START to begin data collection. The device records sensor data for the specified time and transmits it to the smartphone *via* Bluetooth. The raw data are corrected, normalized, and used to calculate the area under the curve (AUC) of sensor responses. These processed values are sent to NGROK via the SEND button, where a machine learning algorithm instantly determines

ammonia concentration, which appears on the screen through the BRING RESULT button. Although a moving average correction algorithm was initially planned to minimize signal fluctuations (Kızıl *et al*., 2015), it was ultimately unnecessary, as meaningful and stable readings were obtained after the first three measurement days.

To ensure that the response graph for each sensor signal reading starts from zero, all values in the series were subtracted from the lowest (first) value. The signals were then normalized using the following equation.

$$S_{norm-t} = \frac{S_t - S_{min}}{S_{max} - S_{min}} \quad \text{(Eq. 1)}$$

In the equation, S_{norm-t} represents the normalized sensor data at second t; S_t represents the sensor data at second t; S_{max} represents the largest sensor reading recorded during the reading; and S_{min} represents the lowest sensor reading recorded during the reading. An example of raw, corrected, and normalized sensor data is given below (Figure 3).

As can be seen in Figure 3 the plot area remains unchanged after approximately 60 seconds, and a plateau phase begins. Therefore, although the device recorded 3 minutes of sniffing, only the first 60 seconds of data were used in the modeling. Next, the areas under the curves (AUC) of the normalized sensor responses were calculated to create a numerical database. The trapezoidal method was applied in the area calculation as follows.

$$\sum AUC = \frac{\Delta_x}{2}[f(x_{i-1}) + f(x_i)] \quad \text{(Eq.2)}$$

The equation represents the mathematical expression for the trapezoidal method used to calculate the area under the curve (AUC). The Δx term in the equation represents the difference between two consecutive measurement points, that is, the step width; this is usually a time difference (e.g., in seconds). $f(x_i)$ and $f(x_{i-1})$ represent the values of the analyzed variable (normalized ammonia value) at the i^{th} and previous measurement points, respectively. When all these small trapezoidal areas are added together, the total area under the entire curve, ∑AUC, is obtained. In this approach, the total area under the curve is equal to the sum of the unit trapezoidal areas.

Laboratory studies

As part of the project, ammonia concentration measurements were first performed with the prototype to be developed in a closed circuit and under controlled conditions. These measurements were compared with gaseous ammonia measurements from parallel experiments held in a conventional boric acid-indicator mixture solution, and the actual ammonia nitrogen values were correlated with the values obtained from E-nose measurements.

The experimental setup was based on a closed (static) chamber system. During e-nose measurements, the jars operated under static conditions without active air recirculation, allowing ammonia released from the soil to accumulate in the headspace. The e-nose device sampled this headspace air directly for concentration-based measurements. Each experimental jar had an approximate total volume of 1 L, providing a defined headspace above the soil samples. Soil-containing Falcon tubes were placed inside the jars without obstructing gas diffusion.

For reference measurements, a dynamic airflow system was applied after each measurement period. Ammonia accumulated in the jars was transferred using a controlled air pump (2×3.5 l/min flow rate) into a boric acid–indicator solution (typically 2% boric acid, volume: 30 mL). The trapped ammonia was subsequently quantified by titration with standardized sulfuric acid according to the method of Bremner (1965).

Thus, the experimental procedure combined a static chamber approach for sensor measurements with a dynamic trapping system for reference quantification, ensuring both controlled sensing conditions and reliable analytical validation. It should be noted that the experimental design combines two different measurement principles: static chamber sensing for the electronic nose and dynamic airflow trapping for the reference method. These approaches inherently differ in their effect on ammonia volatilization. In static chambers, the absence of airflow allows NH_3 to accumulate in the headspace, which may lead to partial saturation and a reduction in the volatilization rate due to decreased concentration gradients. In contrast, the dynamic airflow system continuously removes NH_3 from the chamber, maintaining a higher concentration gradient and promoting sustained volatilization. These methods were not intended to produce directly comparable emission values under identical physical conditions. Instead, the static chamber configuration was used to capture short-term concentration dynamics for sensor analysis, while the dynamic system was used to obtain cumulative NH_3–N values for reference quantification. To enable comparison, sensor responses were integrated over time (AUC), providing a cumulative exposure metric that can be related to total ammonia loss measured by the trapping method.

In this study, each jar was defined as the experimental unit. A total of six sampling times (Days 1, 3, 7, 14, 21, and 28) with three replicates per sampling time were used, resulting in 6 × 3 = 18 jars for each experimental configuration.

For these procedures, a new modified method suitable for the infrastructure in our laboratory was developed under soil conditions, utilizing different ammonia measurement methods reported by Yang *et al*. (2019). A preliminary trial was conducted using a commercial e-nose

(DiagNose II), which confirmed the feasibility of ammonia detection and provided reference correlations (R^2 = 0.84-0.96).

Following the development of the e-nose device, its performance was evaluated under controlled soil conditions. Equal amounts of soil (40 g dry weight) with identical properties were placed in Falcon tubes and amended with 1% urea (46% N). The urea application rate was defined on a weight basis (w/w), corresponding to 0.4 g urea per 40 g soil and 2.4 g urea per 240 g soil. This relatively high application rate was intentionally selected to ensure measurable ammonia release under laboratory conditions and to enhance the sensitivity of the sensor-based system.

Water was added to reach field capacity, and the tubes were placed in closed-system jars (Figure 1b). Ammonia volatilization was monitored sequentially on days 1, 3, 7, 14, 21, and 28 using the e-nose. Parallel measurements were conducted using the Kjeldahl distillation method with boric acid trapping to determine NH_3 losses and correlate them with e-nose readings.

Furthermore, in an identical setup (Figure 5), ammonia released from standard NH_3 solutions was directed into boric acid-indicator solution using motorized airflow, and retained NH_3 was quantified by titration with standardized sulfuric acid (Bremner, 1965).

The electronic nose system recorded sensor responses at a temporal resolution of 1 second over a total measurement duration of 180 seconds per sample. However, based on signal stabilization analysis, only the first 60 seconds of data—representing the dynamic response phase—were used for further processing and modeling.

To justify the selection of the 60-second analysis window, a sensitivity analysis was conducted using different time intervals (30 s, 60 s, and 90 s). The results showed that the 60-second window provided the highest predictive performance (R^2 of 0.84) with lower variability compared to shorter (30 s) and longer (90 s) windows.

A comparative sensitivity analysis was conducted using 30 s, 60 s, and 90 s signal windows (Table 2). Although the 90 s window occasionally produced higher peak R^2 values, model performance became substantially more variable across algorithms, indicating reduced robustness and possible overfitting effects during the plateau phase of the sensor response. In contrast, the 60 s window provided the most balanced performance in terms of predictive accuracy, inter-model consistency, and generalization behavior. The 30 s window produced lower predictive performance because the sensor response had not yet fully stabilized. Therefore, the 60 s window was selected for subsequent modeling and analysis.

To enable comparison between the instantaneous concentration-based sensor measurements and the cumulative NH_3 values obtained from the boric acid trapping method, the area under

the curve (AUC) of the normalized sensor response was calculated using the trapezoidal method. The AUC represents the integrated sensor signal over time and is therefore proportional to the total ammonia exposure during the measurement period.

The initial dataset consisted of 120 measurements obtained from all experimental runs. After preprocessing, a total of 94 valid observations were retained. Specifically, measurements were excluded due to incomplete recordings (e.g., interrupted measurements), sensor instability or communication errors, and failure to meet preprocessing quality criteria (e.g., excessive noise or abnormal signal behavior). This stepwise filtering process ensured data consistency and improved the reliability of the modeling dataset.

In addition to AUC, several simple time-domain features were evaluated, including maximum response (peak signal), initial slope (rate of signal increase during the first 10 seconds), and response time (time required to reach 90% of the maximum signal). These features showed consistent relationships with laboratory-measured NH_3 values, confirming the robustness of the sensor response.

Each experimental configuration consisted of two setups: distributed soil volumes (6 × 40 g tubes per jar) and a single bulk soil mass (240 g per jar). After each measurement, NH_3 gas was directed into the boric acid solution *via* controlled airflow and quantified using classical titration methods (Bremner ,1965).

The soils used were collected from the Dardanos Research and Application Farm, Çanakkale Onsekiz Mart University, Faculty of Agriculture, and prepared according to (Müftüoğlu *et al*., 2014). Basic soil properties (pH, EC, organic matter, $CaCO_3$, and texture) were analyzed following the study by Kacar (1986), while field capacity was determined per the Klute's study findings (1986). NH_3–N, total nitrogen, and available NO_3^- and NH_4^+ concentrations were measured using Kjeldahl distillation techniques as described by Bremner and Mulvaney (1982) and Bremner (1965).

Machine learning algorithms and data processing

Data collected through the mobile application were analyzed using various machine learning algorithms after a comprehensive preprocessing phase. Initially, missing data and outlier analyses were performed using box plots and the interquartile range (IQR) method to ensure data reliability. The first reading of each time series was subtracted from subsequent values to eliminate baseline offset, and all data were normalized to a [0,1] range using the min–max normalization method. This preprocessing ensured comparability across samples and prevented scale-related bias.

Subsequently, scatter plots, AUC distributions, and correlation analyses were generated to explore relationships between variables. Although the dataset was limited due to time constraints, it served as a foundation for model evaluation. Eight regression algorithms—Gradient Boosting, XGBoost, Random Forest, MLP, Lasso, Ridge, Kernel Ridge (RBF), and SVR (RBF)—were compared for predicting the AUC–NH_3 relationship. The three top-performing models were further tested as an ensemble model using voting-based regression for improved accuracy.

To enhance performance, feature engineering was applied through polynomial, logarithmic, and trigonometric transformations, enabling the detection of nonlinear and periodic patterns. Finally, Grid Search optimization was used to fine-tune hyperparameters of each model, ensuring optimal predictive performance and improved generalizability of the developed e-nose data analysis framework. The following performance metrics were used to compare the models:

• MAE (Mean Absolute Error): It shows the average of the absolute difference between the actual and predicted results.

• RMSE (Root Mean Squared Error): This is the square root of the mean squared error. Compared to MAE, it is preferred as a secondary error metric because it increases the error coefficient more significantly due to the large error rates.

• MAPE% (Mean Absolute Percentage Error): The average absolute percentage difference between the actual and predicted values.

• R^2 (R-squared): Indicates the extent to which the variance of the dependent variable can be explained by the independent variable.

• CV_R2_Mean: This shows the average R^2 value based on the results of the cross-validation test. This value indicates the generalization performance of the model on a dataset that has never been presented before.

• CV_R2_Std: This is the standard deviation of the R^2 scores based on the cross-validation test results. This shows how the model's performance changes for each dataset.

Cloud-based data transfer and storage

In the developed system, AUC values calculated by the mobile application are transmitted via the internet to NGROK, where ammonia concentrations are determined in ppm using a machine learning algorithm trained in earlier stages. When the user clicks the “GET RESULT” button, the calculated value is sent back to the application interface. NGROK serves as a secure tunneling tool that enables local servers or applications to be accessed externally without complex configurations such as port forwarding or fixed IP setup. By creating a public, SSL-

certified HTTPS URL, NGROK allows rapid and secure communication between mobile applications, local APIs, and IoT devices like the ESP32.

All reading data and results are then automatically stored in Google Sheets via the phone's internet connection. The data transfer occurs through a specific Google Sheets URL, and storage operations are managed using a custom script written in the Google Script platform. This setup enables real-time data recording, easy access to measurement results, and simplified remote monitoring, providing an efficient, cloud-integrated data management solution for the system.

Results and Discussion

Data preprocessing and key findings of ammonia concentration measurements

The e-nose system developed in this study enables real-time monitoring of ammonia (NH_3) volatilization from fertilized soils. To assess performance, 94 valid sensor readings were preprocessed to remove noise, drift, and baseline offsets. Outlier detection using the interquartile range (IQR) and boxplots confirmed high measurement consistency. Time-series data were baseline-corrected and normalized using the min–max method (0–1 range) as illustrated in Figure 3. The trapezoidal method was then applied to calculate the area under the curve (AUC), representing NH_3 volatilization intensity. Strong positive Pearson and Spearman correlations between AUC and laboratory-measured NH_3 concentrations (Figure 6) verified the system's accuracy and its capability to capture both linear and nonlinear volatilization patterns. These correlation values (Figure 6) are significantly higher compared to those reported in studies on similar systems. While the correlation coefficients reported by Kızıl and Lindley (2001) for ammonia measurements from fertilizer samples were in the range of 0.72–0.92, the values obtained in this project approach the upper limit of this range. This is due to the increased sensitivity of modern sensors and the support of machine learning data.

Overall performance of machine learning models

Eight different machine learning algorithms were tested to model the relationship between AUC values and cumulative NH_3 measurements . The calculations were performed on the Google Colab platform. In the first stage, the models were run without data preprocessing, and the results are summarized in Table 3. In this case, the highest R^2 value of 0.6812 was obtained from the MLP model. This value indicates a moderate level of explanatory power and indicates that the raw data is not suitable for direct modeling. The high MAE and RMSE values in Table 2 confirms that the model errors are relatively large.

After data preprocessing, feature engineering, and hyperparameter optimization were applied, the same models were run again (Table 4). As part of the feature engineering process, polynomial transformations (up to second order), logarithmic transformations, and trigonometric transformations were applied to the data. These processes aimed to better capture nonlinear patterns in the models. Furthermore, the hyperparameters of each model were optimized using the Grid Search method. This method systematically scanned the specified hyperparameter space to find the highest-performance combination.

The results presented in Table 4 show a substantial improvement in model performance. After these steps, the Gradient Boosting model showed the highest performance ($R^2 = 0.84$). XGBoost ($R^2 = 0.8122$) and Random Forest ($R^2 = 0.8101$) followed. Specifically, the MAE value of the Gradient Boosting model decreased to 0.8618. This represents an approximately 18% error reduction compared to the MLP model obtained with raw data. This improvement in model performance is presented as a percentage change in Table 5.

It should be noted that although the Gradient Boosting model achieved a high-test performance ($R^2 = 0.84$), the cross-validation results (CV_R2_mean ≈ 0.48 with relatively high standard deviation) indicate potential instability due to the limited dataset size. This discrepancy may be partially explained by the experimental structure, where multiple measurements originate from the same jars and sampling days. As a result, random data splitting may introduce dependencies between training and test sets, leading to optimistic performance estimates.

This limitation is particularly important given the hierarchical structure of the dataset, in which multiple observations are derived from the same experimental units. Therefore, the reported model performance should be interpreted as indicative rather than definitive. Until validated using grouped or independent datasets, the model should be considered a proof-of-concept rather than a fully generalizable predictive tool. Future studies should implement group-based cross-validation strategies (e.g., grouping by jar or sampling day) to ensure strict independence between training and validation data.

These results clearly demonstrate the critical role of preprocessing and feature engineering in modeling environmental sensor data with machine learning algorithms. Boosting-based methods, particularly Gradient Boosting, can demonstrate strong generalization performance even on relatively small datasets.

In-depth analysis of the gradient boosting model

The Gradient Boosting algorithm was chosen because it can learn complex nonlinear relationships even on relatively small datasets. This model is an ensemble model created by

sequentially training many weak estimators (decision trees). Each new tree learns by reducing the error terms of the previous model. This incremental learning structure is highly effective for capturing small variations in signals such as the NH_3-AUC relationship.

The prediction and error distributions of the Gradient Boosting model are presented in Figure 8. The results indicate that the majority of predictions are closely aligned with the 1:1 reference line, demonstrating strong agreement between predicted and observed values. The error distribution shown in Figure 8 is centered near zero, although a slight negative bias is observed, indicating a minor tendency toward underestimation.

The high performance of boosting algorithms on environmental sensor data has been repeatedly demonstrated in the literature. For example, Wang *et al*. (2018) applied the XGBoost and Gradient Boosting models to predict rice leaf area index using hyperspectral data and reported an R^2 value of 0.82 for the XGBoost model. The R^2 value (0.84) obtained in this project is consistent with, and in some cases even higher than, the performance levels in similar literature studies. This can be explained by the good processing of the time-series features of the sensor-based data.

Performance of the ensemble (voting-based) model

The first three high-performing models (Gradient Boosting, XGBoost, and Random Forest) were combined with a Voting Regressor approach. The performance of all models is comparatively illustrated in Figure 7, based on R^2 values. This method aims to provide more stable overall prediction performance by combining the predictions of the individual models. The R^2 value of the integrated model was calculated as 0.8282. Although this value is slightly lower than the Gradient Boosting model, it provides a more stable and balanced error distribution. A comparative graph of all models based on the R^2 performance metric is presented in Figure 7.

While Gradient Boosting was the most successful method, the integrated model's performance was found to be higher than the other baseline models. Error and prediction distributions for Gradient Boosting are presented in Figure 8.

Examining Figure 8 shows that the model's prediction distribution is generally consistent with the actual results, but there are deviations in some cases. This is also observed in the error distribution. A model performing optimally would be expected to have a normal distribution starting from the center indicated by the red line in the figure. Also Figure 8 shows the model error distribution, while close to the desired optimum, has shifted to the left. The small

deviations in both graphs can be explained by the insufficient number of data and parameters in the dataset.

However, overall, despite the limited dataset, after the preprocessing, feature engineering, and hyperparameter optimization steps, the models appear to have high performance in predicting the AUC-NH_3 relationship. This demonstrates the potential for high performance of these models in datasets with larger data and parameters.

This result is particularly important in field conditions where sensor data can be noisy and variable. Choosing a combined model rather than relying on a single model can increase the system's generalization ability. Similarly, Balasubramanian *et al*. (2005) showed that combining multiple models to estimate electronic nose data in the food industry reduces error variance.

Comparison of findings with literature

Although direct flux measurements provide absolute emission values, concentration-based approaches under controlled conditions can offer a practical and rapid alternative for comparative assessment of ammonia volatilization, particularly when supported by reference methods. It should be emphasized that no direct ammonia emission flux (e.g., mass per unit area per unit time) was calculated in this study. The developed system measures ammonia concentration in the chamber headspace, and the AUC-derived values represent a cumulative proxy for volatilization rather than a true emission rate. It is known that ammonia volatilization rates from soil after urea fertilization are reported in the literature over a wide range. Terman (1980) reported this rate in the range of 30-70%, Torello *et al*. (1983) in the range of 5-10% under field conditions, and Rochette *et al*. (2009) in the range of 10-45% within 10 days. The ammonia losses measured in the trials conducted in this project are consistent with these ranges and confirm the measurement capability of the system. Furthermore, Wang *et al*. (2021) reported that cumulative NH_3 losses in rice fields constitute 9-60% of total nitrogen; these project findings are also consistent with this literature range.

From the first day of the study, in addition to NH_3 losses, nitrogen forms such as NO_3 and NH_4 were also detected. Considering the total nitrogen analyses on the reported days, it was observed that total UREA nitrogen conversions began immediately on the first day, reaching the highest NH_3 concentration value on the 14^{th} day. In our study, a general average loss/conversion of 35.49% of the initial nitrogen value was calculated from the UREA nitrogen. While this amount is in line with the literature, more than one-third of conventional nitrogen fertilizers, especially if not applied at the appropriate time, are no longer beneficial to the plant due to leaching or

ammonia losses. Due to this problem, various nitrogen fertilizers, referred to as slow-release or smart fertilizers, have begun to appear on the market.

In recent years, electronic nose systems have gained increasing interest, particularly in monitoring agricultural gas concentrations. Kızıl and Lindley (2001) and Kızıl (2006) estimated NH_3 concentrations in manure with high correlation coefficients using metal oxide sensors. Markom *et al*. (2007) demonstrated the field usability of low-cost sensors. The MICS-6814 MOS sensor and Bluetooth/Wi-Fi-based data transfer infrastructure used in this study offer an engineering solution consistent with this literature. Additionally, real-time data transfer from the field to the cloud *via* NGROK has enhanced the system's mobility and integration capabilities.

The use of machine learning algorithms in environmental data modeling studies has increased significantly over the last 10 years. Wang *et al*. (2018) used machine learning to model rice leaf area index, and Yamamoto (2019) used machine learning to model plant physiology. Ramesh and Vydeki (2019) reported high accuracy results from MLP and Random Forest methods for disease detection in rice. The high R^2 value of the Gradient Boosting algorithm used in this project is strongly consistent with these literature trends.

The impact of data preprocessing on model performance in environmental sensor data has been emphasized in many studies. In this project, the R^2 value remained at 0.68 when modeling with raw data, but increased to 0.84 after data preprocessing, a concrete indicator of this effect. Feature engineering significantly increased model performance, especially with nonlinear data structures. This has also been reported by Wang *et al*. (2018) and Gaikwad *et al*. (2021).

Conclusions

The most important outcome of this study is the monitoring of ammonia concentrations with a low-cost, portable, and wireless sensor system. The developed system:

- Can be controlled *via* an Android-based mobile application *via* Bluetooth,
- Data is transferred to the cloud via NGROK,
- Automatic data archiving is possible on Google Sheets,
- Instantaneous NH_3 concentration estimation can be made using AUC values.
- The developed system is particularly suitable for controlled laboratory studies and comparative analyses, but its direct application to field-scale emission flux measurements requires further methodological development and validation.

This infrastructure makes it possible to collect data simultaneously from multiple locations in the field and provide instantaneous estimations. Compared to commercial sensor systems, it offers both a cost advantage and a domestic solution thanks to its Turkish interface and open-source software infrastructure.

Measurements conducted under laboratory conditions demonstrated high system repeatability. The absence of outliers in the dataset demonstrates that the sensors' stability and reliability are within acceptable limits. Furthermore, the fact that AUC values mostly reach a plateau within the first 60 sec of the sensor sniffing period suggests that shorter measurement times may be sufficient for field applications. This will increase the system's energy efficiency and enable longer-term data collection.

As with any scientific study, this project has some limitations. First, the dataset size is relatively limited. This may have partially reduced the model's generalization capacity, especially at extreme values. Furthermore, using only the MICS-6814 sensor may limit the model's sensitivity in environments with more complex gas compositions. Integrating different sensors (e.g., NH_3-specific electrochemical sensors) into the system in the future could increase model accuracy.

Furthermore, all of the models used in this study are based on the supervised learning paradigm. In future stages, semi-supervised or deep learning-based approaches (e.g., LSTM or Transformer architectures) can be used to more robustly model time-dependent volatilization trends. This will allow the system to gain not only prediction but also forecasting capabilities.

Finally, the current system is designed to perform measurements at a fixed point. Future projects aim to transform the system into a widespread sensor network by adding LoRaWAN or 4G/NB-IoT infrastructure. This will enable field-based ammonia loss maps to be generated, making fertilization management more precise and environmentally friendly.

This study demonstrated that ammonia volatilization due to nitrogen fertilization in agricultural production can be accurately and reliably estimated using low-cost sensor technology and machine learning models. The high AUC–NH_3 correlation confirms the utility of the MICS-6814 sensor in such studies. The Gradient Boosting model's R^2 value of 0.84, which performs on par with or exceeds similar modeling studies in the literature, demonstrates the power of data preprocessing. The NGROK and Google Sheets-based cloud infrastructure ensured easy field use of the system.

With these features, the developed system can be considered an important tool for both academic research and farm applications as a domestic, low-cost, portable, and highly accurate ammonia monitoring technology.

References

Alfaro M, Salazar F, Hube S, Ramírez L, Mora MS, 2018. Ammonia and nitrous oxide emissions as affected by nitrification and urease inhibitors. J Soil Sci Plant Nutr 18:479–486.

Bremner JM, 1965. Nitrogen availability indexes – chapter 88. In: AG Norman (ed.), Methods of soil analysis. Part 2. Chemical and microbiological properties. Madison, American Society of Agronomy.

Bremner JM, Mulvaney CS, 1982. Nitrogen-total – chapter 31. In: AL Page, MR Miller, DR Keeney (eds.), Methods of soil analysis: Part 2. Chemical and microbiological properties, 9.2.2. (2nd ed.). Madison, American Society of Agronomy.

Brentrup F, Pallière B, 2011. Nitrogen use efficiency as an agro-environmental indicator. Yara International Research Centre. Available from: https://www.yara.com

Burnette E, 2010. Hello, Android: Introducing Google's mobile development platform (3rd ed.). Flower Mound, The Pragmatic Bookshelf.

Denmead OT, 2008. Approaches to measuring fluxes of methane and nitrous oxide between landscapes and the atmosphere. Plant Soil 309:5-24.

Fan JC, Yang WJ, Wu MF, Liu CH, 2006. Determination and analysis of interrill erosion of a soil with coarse fragments in Thailand. T ASABE 49:1305-1314.

Gaikwad SV, Vibhute AD, Kale KV, Mehrotra SC, 2021. An innovative IoT based system for precision farming. Comput Electron Agr 187:106291.

Götze H, Brokötter J, Frößl J, Kelsch A, Kukowski S, Pacholski AS, 2025. Assessment of different methods to determine NH_3 emissions from small field plots after fertilization. Environments 12:255.

Holla S, Katti MM, 2012. Android based mobile application development and its security. Inte J Comput Trends Technol 3:486-490.

IMARC, 2024. Urea market size, share, trends and forecast by grade, application, end-use industry, and region, 2025–2033. Available from: https://www.imarcgroup.com/urea-market

Insausti M, Timmis R, Kinnersley R, Rufino MC, 2020. Advances in sensing ammonia from agricultural sources. Sci Total Environ 706:135124.

IPCC, 2006. 2006 IPCC Guidelines for National Greenhouse Gas Inventories. Volume 4 Agriculture, Forestry and Other Land Use. Available from: https://www.ipcc-nggip.iges.or.jp/public/2006gl/vol4.html

Kacar B, 1986. [Gübreler ve gübreleme tekniği (Fertilizers and fertilization techniques)].[Book in Turkish]. Republic of Turkey Ziraat Bank Cultural Publications.

Kızıl Ü, 2006. Livestock facilities assistance program: a progress report. Dickinson Research Extension Center, North Dakota State University.

Kızıl Ü, Genç L, Rahman S, Khaitsa ML, Genc TT, 2015. Design and test of a low-cost electronic nose system for identification of Salmonella enterica in poultry manure. T ASABE 58:819-826.

Kızıl Ü, Lindley JA, 2001. Comparison of different techniques in the determination of animal manure characteristics. Proc. ASAE/CSAE North Central Sections Conference, Brookings.

Klute A, 1986. Methods of soil analysis. Part 1: Physical and mineralogical methods (2nd ed.). Madison, American Society of Agronomy.

Li T, Wang C, Ji W, Wang Z, Shen W, Feng Y, Zhou M, 2023. Cutting-edge ammonia emissions monitoring technology for sustainable livestock and poultry breeding: A comprehensive review of the state of the art. J Clean Prod 428:139387.

Markom MA, Md Shakaff AY, Adom AH, Fikri NA, Khan SF, Abdullah AH, Isa, C.M.N.C. 2007. Development of low cost electronic nose. Research Report. Universiti Malaysia Perlis.

Müftüoğlu NM, Türkmen C, Çıkılı Y, 2014. [Toprak ve bitkide verimlilik analizleri (Soil and plant productivity analyses)].[Book in Turkish]. Nobel Academic Publishing.

Okur N, 2021. [Toprak bilimi ve bitki besleme (Soil science and plant nutrition)].[Book in Turkish]. Nobel Academic Publishing.

Pocatilu P, 2011. Android applications security. Info Econ 15:163-171.

Polat H, 2018. [Türkiye tarım topraklarının verimlilik özellikleri (Productivity characteristics of Turkish agricultural lands)].[Book in Turkish]. Turkish Union of Chambers of Agriculture Farmer and Village World Magazine.

Polat H, Güngör İ, Koca C, 2013. [Türkiye'de kullanılan azotlu gübrelerin standart ve yönetmeliklerle uyumluluğu üzerine bir araştırma (A study on the compliance of nitrogen fertilizers used in Turkey with standards and regulations)].[Article in Turkish]. Topraksu Dergisi 2:102-111.

Ramesh S, Vydeki D, 2019. Application of machine learning in detection of blast disease in South Indian rice crops. J Phytol 11:31-37.

Redding MR, Shorten PR, Lewis R, Pratt C, Paungfoo-Lonhienne C, Hill J, 2016. Soil N availability, rather than N deposition, controls indirect N_2O emissions. Soil Biol Biochem 95:288-298.

Rochette P, Macdonald JD, Angers DA, Chantigny MH, Gasser MO, Bertrand N, 2009. Banding of urea increased ammonia volatilization in a dry acidic soil. J Environ Qual 38:1383-1390.

Sintermann J, Spirig C, Jordan A, Kuhn U, Ammann C, Neftel A, 2012. Eddy covariance flux measurements of ammonia by high temperature chemical ionisation mass spectrometry. Atmos Meas Tech 4:599-616.

TAGEM, 2024. [Gübre sektör politika belgesi 2023–2027 (Fertilizer industry policy document 2023-2027)].[Report in Turkish]. Ankara, General Directorate of Agricultural Research and Policies.

Terman GL, 1980. Volatilization losses of nitrogen as ammonia from surface-applied fertilizers, organic amendments, and crop residues. Adv Agron 31:189-223.

Torello WA, Wehner DJ, Turgeon AJ, 1983. Ammonia volatilization from fertilized turfgrass stands. Agronomy J 75:454-456.

Wang C, Sun H, Zhang J, Zhang X, Lu L, Shi L, Zhou S, 2021. Effects of different fertilization methods on ammonia volatilization from rice paddies. J Clean Prod 295:126299.

Wang L, Chang Q, Yang J, Zhang X, Li F, 2018. Estimation of paddy rice leaf area index using machine learning methods. PLoS One 13:e0207624 .

Wang W, Cao J, Zhang R, Chen L, Li Y, Zhang Y, 2024. Design strategies of semiconductor sensors toward ammonia monitoring in smart agriculture. J Environ Chem Eng 12:114380.

Yamamoto, K. 2019. Distillation of crop models to learn plant physiology theories using machine learning. PLoS One 14:e0217075.

Yang W, Que H, Wang S, Zhu A, Zhang Y, He Y, et al., 2019. High temporal resolution measurements of ammonia emissions following different nitrogen application rates from a rice field in the Taihu Lake Region of China. Environ Pollut 257:113489.

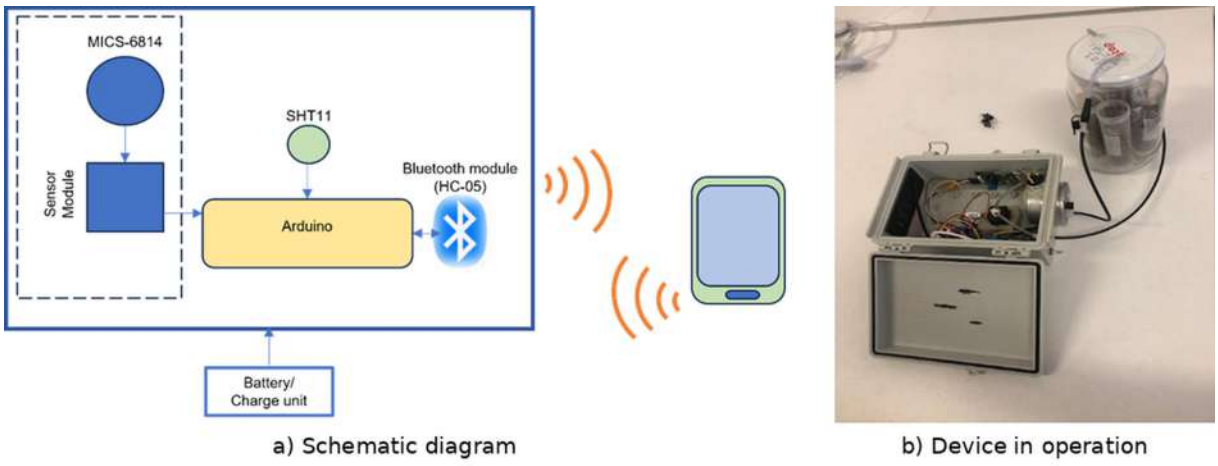

Figure 1. (a) Schematic diagram of the developed e-nose system, (b) prototype device in operation.

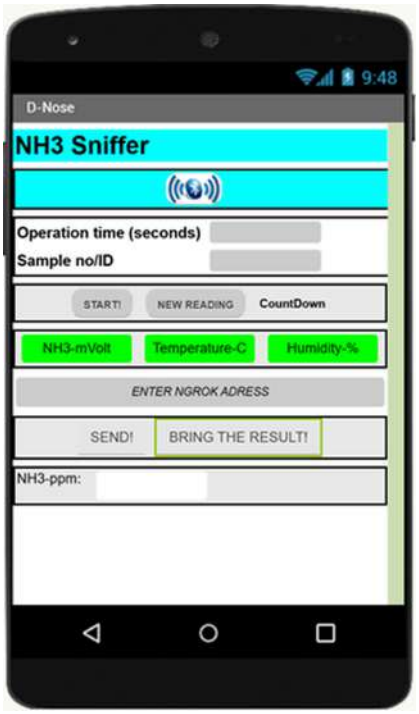

Figure 2. Android application user interface.

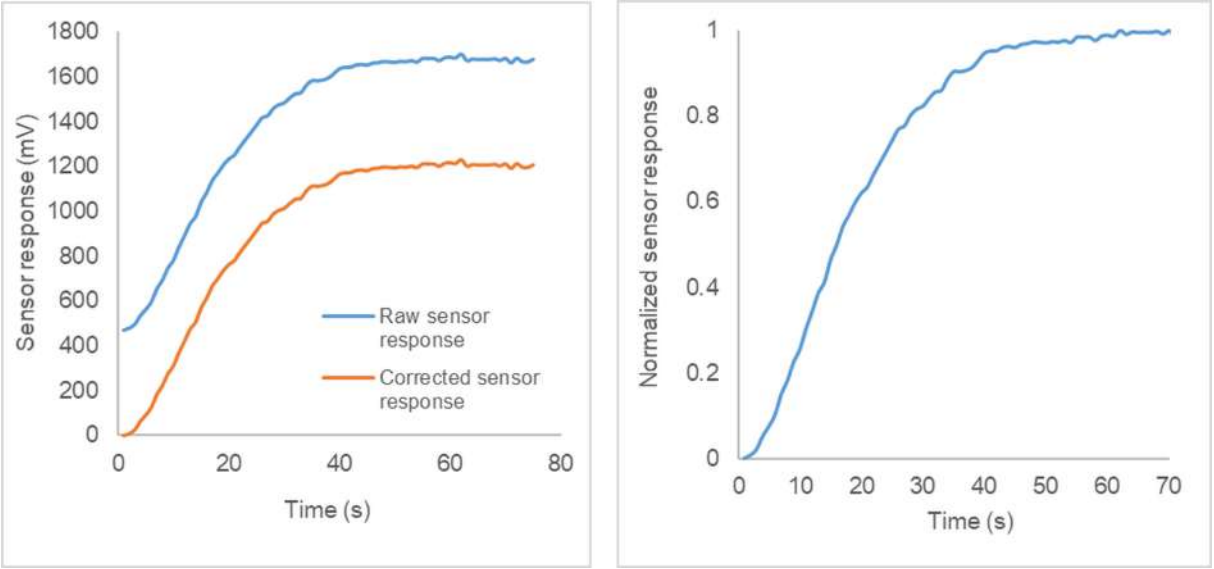

Figure 3. Raw, corrected, and normalized sensor data.

Figure 4. Experimental setup used in the preliminary ammonia measurement trial.

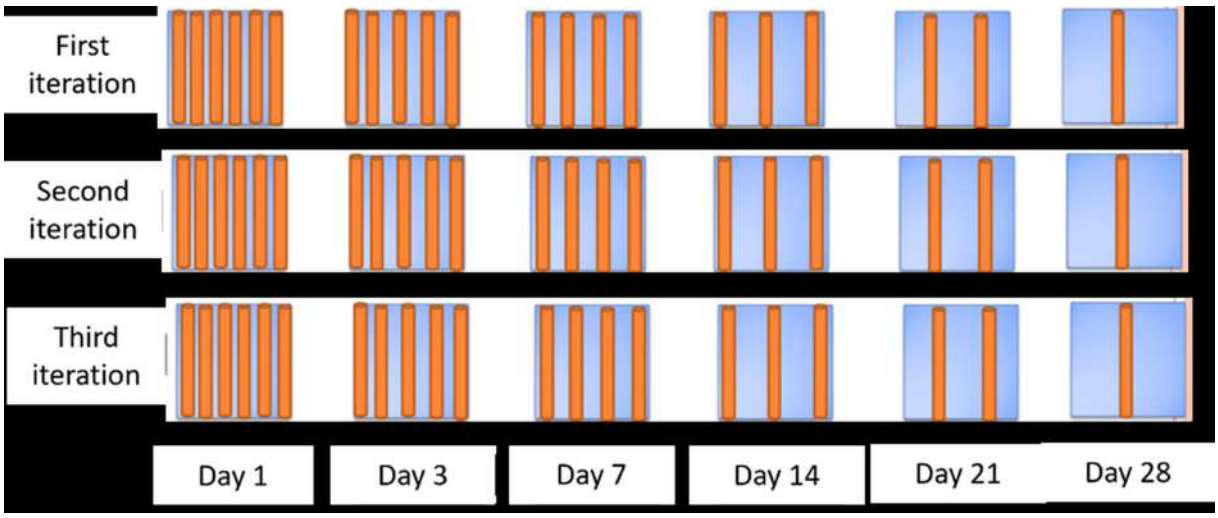

Figure 5. Schematic representation of the experimental setup, including static chamber measurements and dynamic ammonia trapping system.

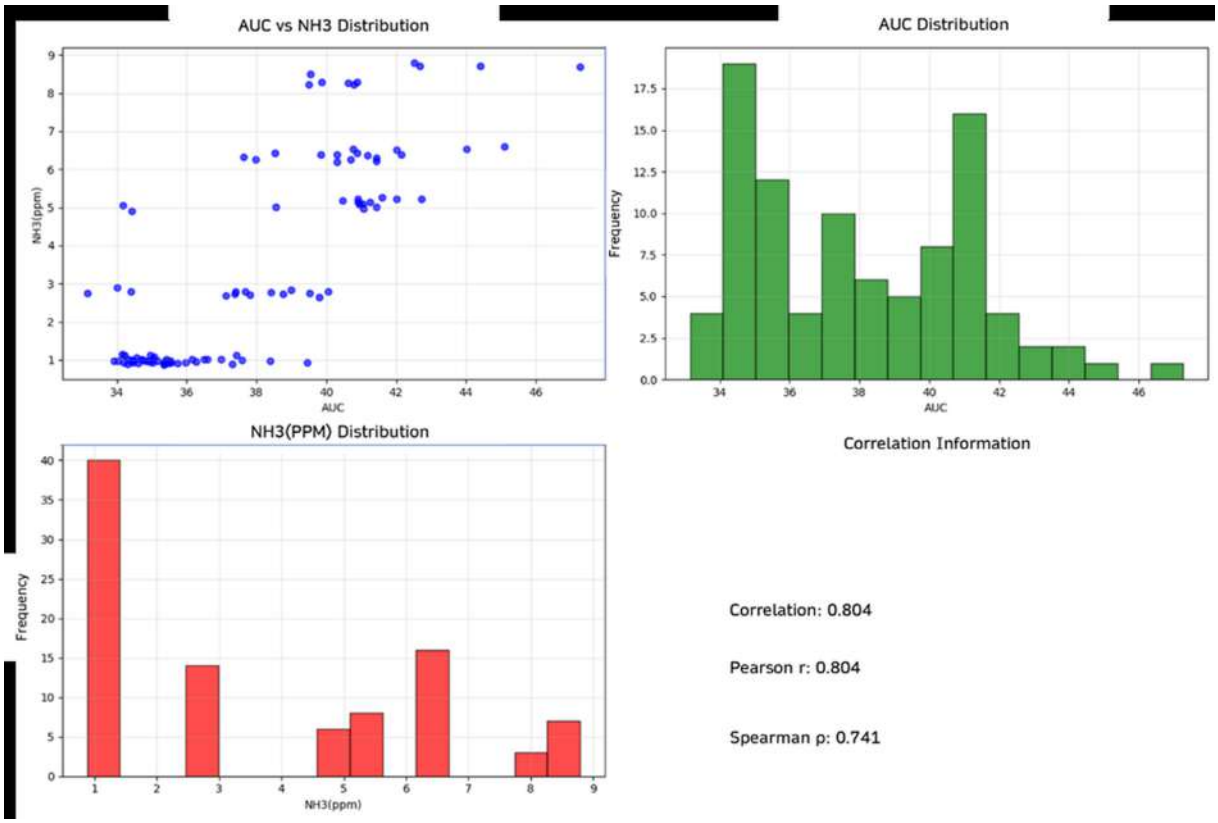

Figure 6. Relationship between AUC values and laboratory-measured NH_3 concentrations, including distribution and correlation analysis.

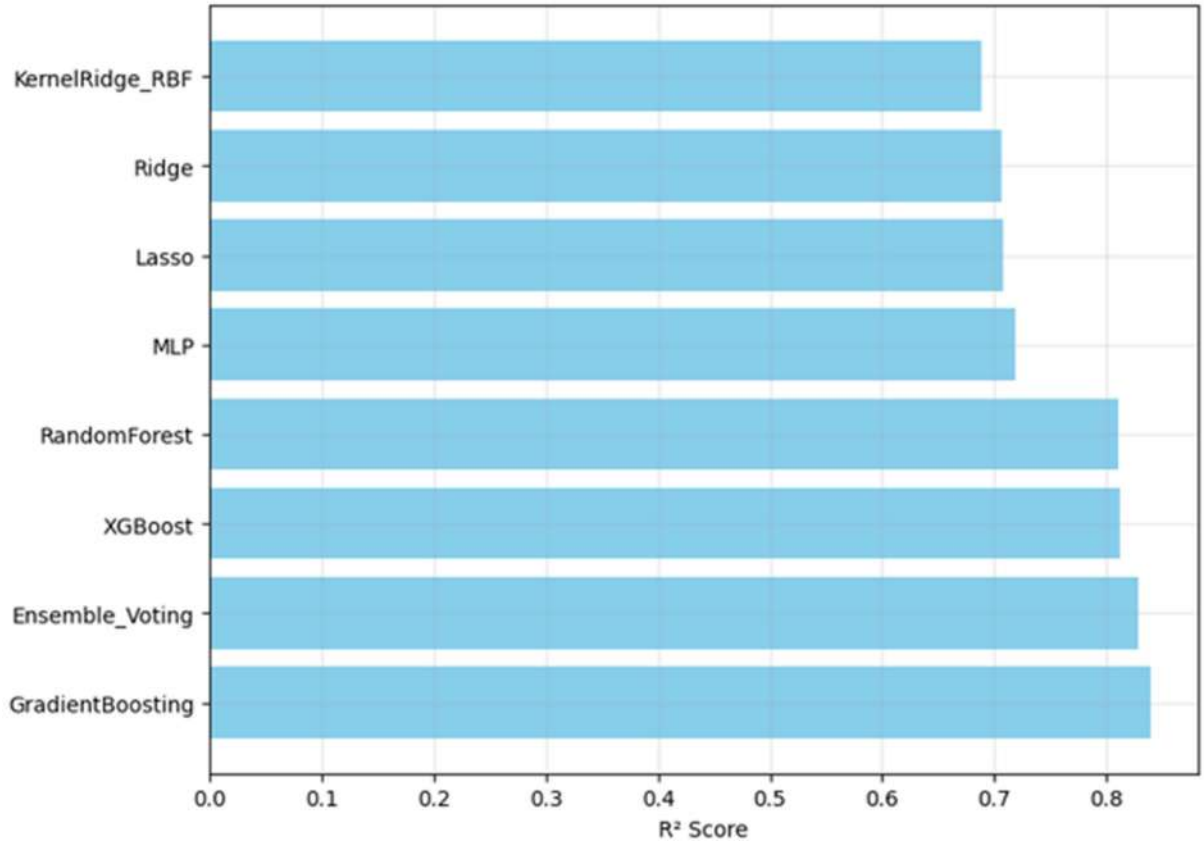

Figure 7. Comparison of model performance based on R^2 values.

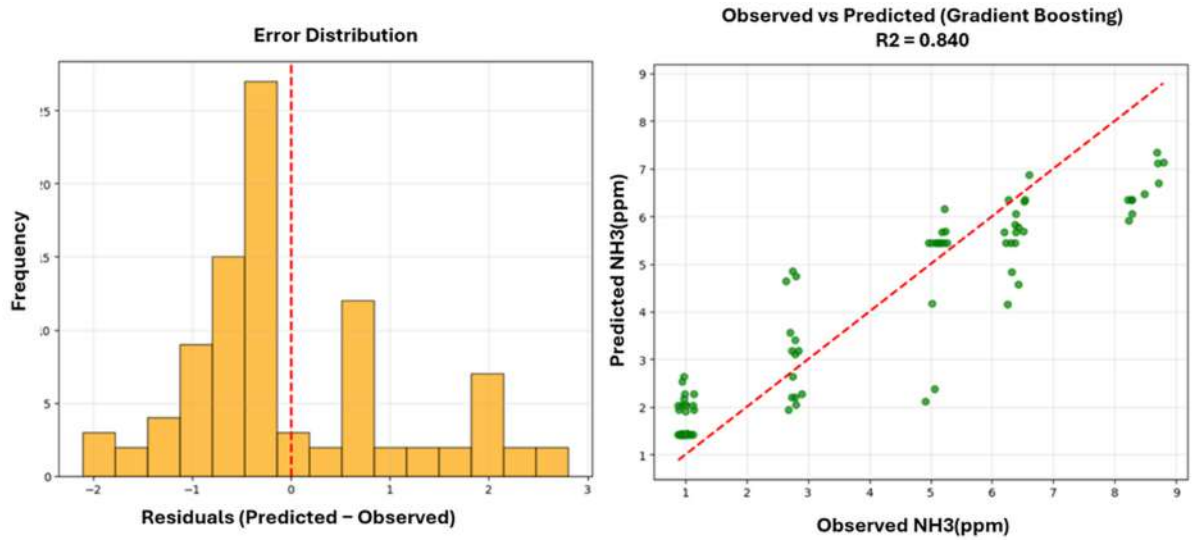

Figure 8. Gradient Boosting model performance: (left) distribution of prediction errors (residuals), (right) observed *vs* predicted NH_3 concentrations.

Table 1. Technical specifications of the sensors used.

Sensor	Type	Target gas / parameter	Detection range	Sensitivity	Resolution
MICS-6814	Metal oxide semiconductor (MOS)	NH_3	~1–500 ppm	Change in resistance proportional to gas concentration (Rs/R0)	Not absolute; depends on calibration curve
SHT11	Digital sensor	Temperature	-40 to +123.8°C	±0.4°C accuracy	0.01°C
SHT11	Digital sensor	Relative humidity	0–100% RH	±3% RH accuracy	0.03% RH

Table 2. Sensitivity analysis of different signal window durations used for AUC calculation and machine learning modeling.

Window duration	Best model	R^2	MAE	RMSE	MAPE (%)	Stability assessment
30 s	Ensemble	0.8729	0.7049	0.9272	26.71	Moderate
60 s	Gradient boosting	0.8400	0.8618	1.0734	40.76	High
90 s	Ensemble	0.9223	0.5828	0.7251	29.95	Low

Table 3. Model performance values before preprocessing steps.

Model	MAE	RMSE	R^2	MAPE (%)
GradientBoosting	1.2784	1.9427	0.4759	52.9597
XGBoost	1.411	2.1698	0.3462	53.7986
RandomForest	1.2666	1.8773	0.5106	53.8856
MLP	1.1212	1.5152	0.6812	46.1168
Lasso	1.6524	1.914	0.4912	88.9255
Ridge	1.2344	1.6146	0.638	55.4782
KernelRidge_RBF	1.146	1.6651	0.615	42.7246
SVR_RBF	1.0884	1.6036	0.6429	36.5079

Table 4. Model performance values after preprocessing steps.

Model	MAE	RMSE	R^2	MAPE(%)	CV_R2_Mean	CV_R2_Std
GradientBoosting	0.8618	1.0734	0.8400	40.7613	0.4824	0.4113
XGBoost	0.9070	1.1631	0.8122	42.7301	0.4893	0.3421
RandomForest	0.8224	1.1695	0.8101	32.4939	0.5125	0.5020
MLP	0.9986	1.4219	0.7192	38.6933	0.5904	0.2977
Lasso	1.0569	1.4493	0.7083	41.9965	0.5881	0.2885
Ridge	1.0676	1.4542	0.7063	42.5471	0.5863	0.2880
KernelRidge_RBF	1.0556	1.4973	0.6887	39.7097	0.5422	0.2608
SVR_RBF	1.1000	1.5127	0.6822	43.1431	0.5968	0.2244

Table 5. The effect of preprocessing steps on model performance.

Model	R^2 (before)	R^2 (after)	ΔR^2	MAE (before)	MAE (after)	MAE reduction (%)
GradientBoosting	0.4759	0.8400	0.3641	1.2784	0.8618	32.59
XGBoost	0.3462	0.8122	0.4660	1.4110	0.9070	35.72
RandomForest	0.5106	0.8101	0.2995	1.2666	0.8224	35.07
MLP	0.6812	0.7192	0.0380	1.1212	0.9986	10.93
Lasso	0.4912	0.7083	0.2171	1.6524	1.0569	36.04
Ridge	0.6380	0.7063	0.0683	1.2344	1.0676	13.51
KernelRidge_RBF	0.6150	0.6887	0.0737	1.1460	1.0556	7.89
SVR_RBF	0.6429	0.6822	0.0393	1.0884	1.1000	-1.07